Langmuir−Blodgett Films of Heteropolyoxometalate/ Organomercury Acetylide Hybrid Composites: Characterization and Photoelectric Properties

Li Liu,* Wei-He Ai, Ming-Jian Li, and Shi-Zhong Liu

Ministry of Education Key Laboratory for the Synthesis and Application of Organic Functional Molecules and School of Chemistry and Chemical Engineering, Hubei University, Wuhan 430062, People's Republic of China

Chun-Mei Zhang, Hong-Xia Yan, and Zu-Liang Du

Key Laboratory of Special Functional Materials, Henan University, Kaifeng, 475001, People's Republic of China

Wai-Yeung Wong*

Department of Chemistry, Hong Kong Baptist University, Waterloo Road, Kowloon Tong, Hong Kong, People's Republic of China

Received November 29, 2006. Revised Manuscript Received February 2, 2007

A new family of organometallic/inorganic nanohybrid Langmuir−Blodgett (LB) films consisting of rigid-rod organomercury acetylide complex (OMA-C_{16} or OMA-C_8) as the π-conjugated organometallic molecule, tungsto(molybdo)phosphoric heteropolyacids HPA (HPA = $H_3PMo_{12}O_{40}$, $H_3PW_{12}O_{40}$, $H_6P_2Mo_{18}O_{62}$, or $H_6As_2W_{18}O_{62}$) of the Keggin and Dawson structures as the inorganic component, and octadecylamine (ODA) as the auxiliary film-forming agent were prepared and characterized by $\pi-A$ isotherms, UV−vis absorption spectra, fluorescence spectra, atomic force microscopy imaging, scanning tunneling microscopy, surface photovoltage spectroscopy, and low-angle X-ray diffraction. Our experimental results indicate that steady, even, and ordered Langmuir and LB films are formed in pure water and heteropolyacid subphase. They typically have a highly organized lamellar structure in which a monolayer of HPA is arranged alternately with well-ordered layers of OMA (and also ODA for OMA-C_{16}) and the periodicity of the layered structure for the OMA-C_{16}/ODA/$H_3PMo_{12}O_{40}$ LB film is ca. 3.7 nm. Luminescence spectra of hybrid LB films show that HPA can quench the emission of OMA-C_{16} and OMA-C_8 to some extent. These LB composites show good photovoltage responses and a photovoltage of 103 μV can be obtained for the OMA-C_{16}/ODA/$H_3PMo_{12}O_{40}$ system when it is excited by light at 330 nm. The monolayer LB films on silica wafer can also display interesting electrical conductivity behavior.

Introduction

The design, synthesis, and structural characterization of new hybrid materials, in which many applications can be predicted through the assembly of organic and inorganic building blocks, is an important current research area in materials science.[1] The construction of such organic/inorganic hybrids is regarded useful for obtaining multifunctional materials with new electrical and/or optical properties.[2] However, while most of the existing materials have been obtained as crystals, they find very limited practical applications. An alternative way in relation to the goal is to prepare these materials as films or nanoparticles or to incorporate them into organic or inorganic matrices.[3]

Langmuir−Blodgett (LB) technique is considered an elegant approach to arrange molecules into well-organized multilayer films.[4] It also allows the processing of molecules in the form of thin films, which are preferred for many applications and permits the control of the two-dimensional structure of these films at the molecular level along with ease of multilayer deposition, compared to other techniques such as spin-cast, vapor deposition, or self-assembled

* To whom correspondence should be addressed. L. Liu: tel., +8627-63422166; fax, +8627-88663043; e-mail, liulihubei@gmail.com. W.-Y. Wong: tel., +852-34117074; fax, +852-34117348; e-mail, rwywong@hkbu.edu.hk.

(1) Hargmann, J. P.; Hargmann, D.; Zubieta, J. *Angew. Chem., Int. Ed.* **1999**, *38*, 2638.

(2) (a) Awaga, K.; Coronado, E.; Drillon, M. *MRS Bull.* **2000**, 52. (b) Clave, A. E.; Coronado, E.; Galán-Mascarós, C. J.; Gómez-García, C. J.; Laukkhin, V. *Nature* **2000**, *408*, 447. (c) Coronado, E.; Day, P. *Chem. Rev.* **2004**, *11*, 5419. (d) Coronado, E.; Galán-Mascarós, C. J. *J. Mater. Chem.* **2005**, *15*, 66.

(3) (a) Ying, J.-W.; Sobransingh, D. R.; Xu, G.-L.; Kaifer, A. E.; Ren, T. *Chem. Commun.* **2005**, 357. (b) *Molecular Electronics*; Reed, M. A., Lee, T., Eds.; American Scientific Publishers; Stevenson Ranch, CA, 2003. (c) *Handbook of Nanoscience, Engineering and Technology*; Goddard, W. A., Brenner, D. W., Lysehevski, S. E., Iafrate, G. J., Eds.; CRC Press: Boca Raton, FL, 2003.

(4) (a) Ulman, A. *An Introduction to Ultrathin Organic Films: From Langmuir-Blodgett to Self-assembly*; Academic Press: Boston, 1991. (b) Talham, D. R. *Chem. Rev.* **2004**, *104*, 5479. (c) Kuhn, H.; Möbius, D.; Bücher, H. *Physical Methods of Chemistry, Part IIIB*; Wiley-Interscience: New York, 1972; Chapter VII. (d) Gaines, G. L., Jr. *Insoluble Monolayers at Liquid-Gas Interface*; Wiley-Interscience: New York, 1966.

10.1021/cm062838c CCC: $37.00
Published on Web 03/10/2007

monolayers.[4c,4d] For these reasons, the LB method has been widely applied to make ultrathin films with a specific architecture which can be exploited as chemo- or biosensors, modified electrodes, optical logic gates, or molecular electronic devices.[4,5]

Polyoxometalate anions (POMs) represent a class of inorganic compounds that thanks to their topological and electronic versatilities have found wide applications in catalysis, biology, medicine, and materials science.[6,7] Remarkably, they can act as electron reservoirs and are reversibly reduced readily by the addition of various numbers of electrons to give mixed-valence species. Their solubility and chemical stability in both aqueous and nonaqueous solvents make them very useful as the inorganic components of functional molecular materials.[8]

Since the work of Clemente-León and his co-workers in the preparation of inorganic/organic hybrid LB films using heteropolyacid and surfactant DODA (DODA = dimethyldioctadecylammonium) as film materials,[9] research work in this field is continuously expanding and has mainly focused on the study of magnetic, electrochemical, and electrochromic properties of inorganic/organic hybrid LB films in which the organic surfactant is embedded in heteropolyacid with different shape, size, and charge.[8] While the cationic surfactant plays only a structural role, the electronic properties of POM-based LB films are principally governed by the POMs. Another attractive method depends on creating novel hybrid LB films that combine the properties of both the inorganic entities and the organic component of the film. With this idea in mind, an organomercury acetylide complex (OMA) that can introduce electronic delocalization within the LB film was designed by us and it can be combined with electron reservoir POMs and/or amphiphilic octadecylamine (ODA) to prepare a new type of hybrid organometallic/inorganic LB films. While Langmuir and Langmuir−Blodgett films of a great variety of molecular metal complexes with interesting magnetic or optical properties have been prepared in the past few years,[10] to our knowledge, the use of mercury-derived compounds in LB film preparation is very rare.[11] As far as we know, self-assembly of group 12 mercury acetylide in forming LB film by the LB technique has not been reported previously. They are expected to have functional potential as a component of luminescent film devices. With our growing interests in the design and synthesis of luminescent functional materials of group 10−12 metallaynes,[12] we report here the first examples of the preparation of OMA/HPA hybrid LB films in the presence or absence of ODA and their structures and photovoltaic behavior are discussed in detail. A monolayer of ODA essentially serves as the auxiliary film-forming agent here and can be used as a template for adsorption of various POMs.

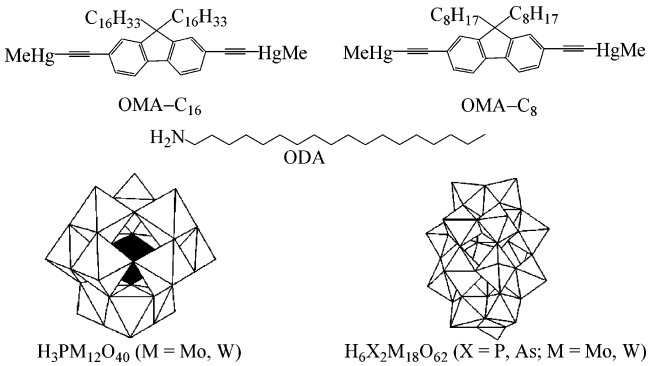

Figure 1. Molecular structure of compounds used in the construction of hybrid LB films.

Experimental Section

Materials. Four types of HPA, viz. $H_3PMo_{12}O_{40}$, $H_3PW_{12}O_{40}$, $H_6P_2Mo_{18}O_{62}$, and $H_6As_2W_{18}O_{62}$ (denoted as $HPMo_{12}$, HPW_{12}, HP_2Mo_{18}, and HAs_2W_{18}, respectively) and the organomercury acetylide (OMA) coordinated with the 9,9-dioctylfluorene-2,7-diacetylide (OMA-C_8) and 9,9-dihexadecylfluorene-2,7-diacetylide (OMA-C_{16}) chromophores were synthesized according to the procedures previously reported.[13,14] Octadecylamine and chloroform were used as received without further purification.

Monolayer and LB Film Fabrication. The formulas of the composites for the LB films are shown in Figure 1. HPA can be organized as monolayers using the LB technique. Monolayer formation and deposition were carried out on a French LB 105 slot under room-temperature condition at 20 ± 1 °C. The surface pressure was measured by the Wilhelmy method. Triple-distilled deionized water (pH = 6) was used as the subphase. The spreading solution of OMA-C_{16} and ODA (1:1, 1×10^{-3} mmol dm^{-3}) in

(5) (a) Ide, M.; Mitamura, A.; Miyashita, T. *Bull. Chem. Soc. Jpn.* **2001**, *74*, 1355. (b) Kado, Y.; Aoki, A.; Miyashita, T. *Int. J. Nanosci.* **2002**, *5*−*6*, 637. (c) Chu, B. W.-K.; Yam, V. W.-W. *Langmuir* **2006**, *22*, 7437. (d) Amao, Y.; Asai, K.; Miyashita, T.; Okumura, I. *Polym. J.* **1999**, *31*, 1267. (e) Amao, Y.; Asai, K.; Miyashita, T.; Okumura, I. *Polym. Adv. Technol.* **2000**, *11*, 705. (f) Aoki, A.; Miyashita, T. *Macromolecules* **1996**, *29*, 4662. (g) Fukuda, N.; Mitsuishi, M.; Miyashita, T. *J. Phys. Chem. B* **2002**, *106*, 7048. (h) Matsui, J.; Mitsuishi, M.; Aoki, A.; Miyashita, T. *Angew. Chem., Int. Ed.* **2003**, *42*, 2272. (i) Matsui, J.; Mitsuishi, M.; Aoki, A.; Miyashita, T. *J. Am. Chem. Soc.* **2004**, *126*, 3708.

(6) Pope, M. T.; Müller, A. *Angew. Chem., Int. Ed. Engl.* **1991**, *30*, 34.

(7) *Polyoxometalates: From Platonic Solids to Anti-Retroviral Activity*; Pope, M. T., Müller, A., Eds.; Kluwer Academic Publishers; Dordrecht, 1994; Vol. 10.

(8) Clemente-León, M.; Coronado, E.; Gómez-García, C. J.; Mingotaud, C.; Ravaine, S.; Romualdo-Torres, G.; Delhaès, P. *Chem. Eur. J.* **2005**, *11*, 3979.

(9) (a) Clemente-León, M.; Mingotaud, C.; Agricole, B.; Gómez-García, C. J.; Coronado, E.; Delhaes, P. *Angew. Chem., Int. Ed. Engl.* **1997**, *36*, 1114. (b) Clemente-León, M.; Agricole, B.; Mingotaud, C.; Gomez-Garcia, C. J.; Coronado, E.; Delhaes, P. *Langmuir* **1997**, *13*, 2340.

(10) Clemente-León, M.; Coronado, E.; Soriano-Portillo, A.; Mingotaud, C.; Dominguez-Vera, J. M. *Adv. Colloid Interface Sci.* **2005**, *116*, 193.

(11) (a) Elliot, D. J.; Furlong, D. N.; Gengenbach, T. R.; Grieser, F. *Collids Surf., A* **1995**, *102*, 45. (b) Lee, K.-J.; Kim, K.-H.; Kim, S.-R.; Tae, G.-Y.; Kim, J.-D. *Synth. Met.* **1993**, *55*−*57*, 3848.

(12) (a) Wong, W.-Y.; Ho, C.-L. *Coord. Chem. Rev.* **2006**, *250*, 2627 and references therein. (b) Wong, W.-Y. *J. Inorg. Organomet. Polym. Mater.* **2005**, *15*, 197. (c) Wong, W.-Y. *Comment Inorg. Chem.* **2005**, *26*, 39. (d) Zhou, G.-J.; Wong, W.-Y.; Lin, Z.; Ye, C. *Angew. Chem., Int. Ed.* **2006**, *45*, 6189. (e) Manners, I. *Synthetic Metal-containing Polymers*; Wiley-VCH: Weinheim, 2004; Chapter 5, p 153. (f) Nguyen, P.; Gómez-Elipe, P.; Manners, I. *Chem. Rev.* **1999**, *99*, 1515. (g) Abd-El-Aziz, A. S. *Macromol. Rapid Commun.* **2002**, *23*, 995.

(13) Wu, T.-H.; Li, J.-Q.; Yang, H.-M.; Wang, G.-J.; Zhang, H.-B.; Wei, Q.; Jiang, Y.-Z. *Chem. J. Chin. Univ.* **1991**, *12*, 1373.

(14) (a) Liu, L.; Chen, Z.-X.; Liu, S.-Z., Wong, W.-Y. *Acta Chim. Sinica* **2006**, *64*, 884. (b) Wong, W.-Y.; Choi, K.-H.; Lu, G.-L.; Shi, J.-X.; Lai, P.-Y.; Chan, S.-M.; Lin, Z. *Organometallics* **2001**, *20*, 5446. (c) Liu, L.; Li, M.-X.; Wong, W.-Y. *Aust. J. Chem.* **2005**, *58*, 799. (d) Liu, L.; Ho, C.-L.; Wong, W.-Y. *Aust. J. Chem.* **2006**, *59*, 434. (e) Wong, W.-Y.; Liu, L.; Shi, J.-X. *Angew. Chem., Int. Ed.* **2003**, *42*, 4064.

chloroform was spread onto the pure water subphase using a microsyringe; when the solvent had evaporated thoroughly, compression began with the compression rate at 10 cm^2 min^{-1} and the curve was recorded. The procedure of LB film fabrication was essentially the same as that for the monolayer except that the subphase is HPA aqueous solution (1×10^{-6} mol L^{-1}). All the experiments for monolayer deposition were performed under a surface pressure of 30 mN m^{-1}. ODA plays only a structural role in ensuring a good-quality LB film for OMA-C_{16} and it was observed that the organization of HPA molecules within the LB films is not so good without the ODA monolayer. But for OMA-C_8, we can obtain reasonable OMA-C_8/HPA LB films without the addition of ODA. In the case where a stable Langmuir monolayer of OMA-C_{16}/ODA or OMA-C_8 was formed on the subphase, the monolayer was subsequently deposited onto ITO or quartz substrates by the vertical dipping method at a rate of 1 mm min^{-1}, resulting in a fairly good deposition of a typical Y-mode film. The number of layers of LB film prepared here is equal to the number of dipping or lifting processes, on each of which a floating Langmuir monolayer was transferred onto the substrate with a good transfer ratio.

Instruments. Ultraviolet−visible (UV−vis) spectra were measured on a UNICAM Heλios α spectrometer. Low-angle X-ray diffraction measurements were carried out on a Philips X'pert Pro instrument, operating with a monochromated Cu Kα radiation source at 40 kV and 50 mA. Surface photovoltage spectroscopy was measured on a D-300 surface photovoltage instrument. Photoluminescence spectra were recorded on a SPEX F212 fluorescence spectrometer. AFM image and scanning tunneling microscopy of the LB films were measured on a SPA-400 atomic force microscope.

Results and Discussion

Synthesis. The organometallic mercury complexes OMA-C_{16} and OMA-C_8 were prepared in good yields by the direct base-catalyzed mercuration of 2,7-diethynyl-9,9-dihexadecylfluorene and 2,7-diethynyl-9,9-dioctylfluorene with 2 equiv of MeHgCl at room temperature according to the published procedures.[14a,e] These compounds are readily soluble in chlorinated solvents such as $CHCl_3$ and CH_2Cl_2 to give a pale yellow solution. The long hydrocarbon chains are attached to the fluorene ring to enhance the solubility of the complex. The OMA complex shows a single ^{199}Hg NMR peak at around δ −453 (versus δ −847 for MeHgCl), reflecting polarization of the Hg−C≡ bond.

Surface Pressure−Area Isotherms. Figure 2 shows the surface pressure−area (π−A) isotherms of OMA-C_{16}/ODA and OMA-C_8 on HPA and the pure water subphase solutions at 20 °C. The results show that they can form stable monolayer Langmuir film at the air−liquid interface. The molecular area of OMA-C_{16}/ODA and OMA-C_8 on the HPA aqueous solutions and pure water can be estimated by extrapolating the line part of π−A isotherm to the abscissa. The relevant data are displayed in Table 1. The isotherm is progressively modified by using different HPA polyoxoacids. For OMA-C_{16}/ODA film spread on the pure water subphase, for instance, the limiting area per molecule is 0.35 nm^2, whereas that of OMA-C_{16}/ODA in HPA aqueous subphase is 0.50−0.55 nm^2. The collapse pressure of OMA-C_{16}/ODA in HPA aqueous solution is 32.6−33.4 mN m^{-1}, slightly larger than that in water phase (31.1 mN m^{-1}). Apparently,

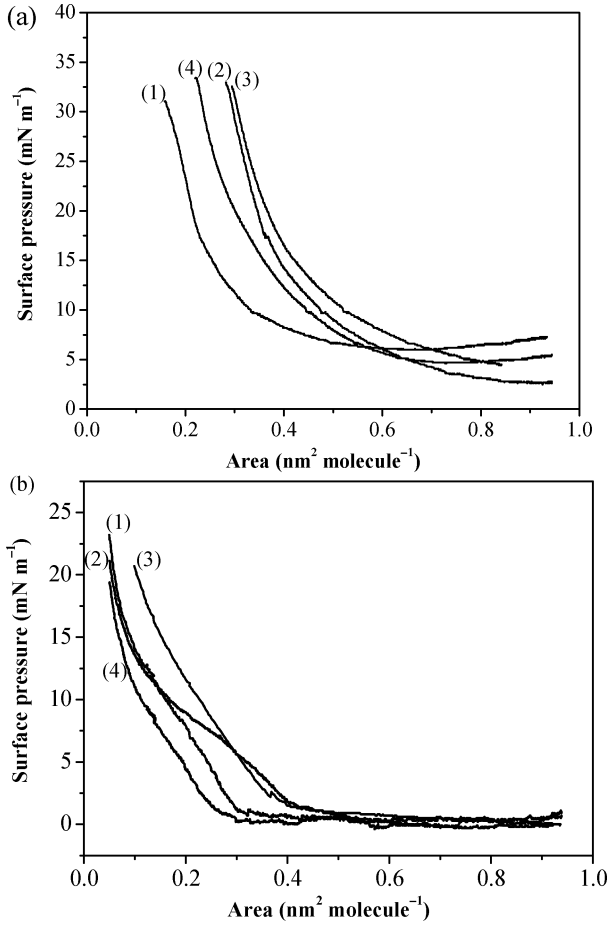

Figure 2. Surface pressure−area (π−A) isotherms of (a) monolayer films of (1) OMA-C_{16}/ODA/H_2O, (2) OMA-C_{16}/ODA/$HPMo_{12}$, (3) OMA-C_{16}/ODA/HP_2Mo_{18}, and (4) OMA-C_{16}/ODA/HPW_{12} and (b) monolayer films of (1) OMA-C_8/H_2O, (2) OMA-C_8/$HPMo_{12}$, (3) OMA-C_8/HP_2Mo_{18}, and (4) OMA-C_8/HAs_2W_{18}.

Table 1. Surface Pressure−Area Isotherm Data of the LB Films

film	solid-state region (mN m^{-1})	cross section (nm^2 $molecule^{-1}$)	collapse pressure (mN m^{-1})
OMA-C_{16}/ODA/H_2O	17.3−31.1	0.35	31.1
OMA-C_{16}/ODA/$HPMo_{12}$	17.6−32.9	0.54	32.9
OMA-C_{16}/ODA/HP_2Mo_{18}	21.4−32.6	0.55	32.6
OMA-C_{16}/ODA/HPW_{12}	24.9−33.4	0.50	33.4
OMA-C_8/H_2O	16.8−23.2	0.23	23.2
OMA-C_8/$HPMo_{12}$	14.6−21.1	0.24	21.1
OMA-C_8/HP_2Mo_{18}	15.0−20.7	0.33	20.7
OMA-C_8/HAs_2W_{18}	10.5−19.4	0.20	19.4

isotherms on HPA aqueous solutions exhibited an increase in the molecular area and surface pressure compared with the case for pure water, suggesting that HPA molecules are not embedded inside the OMA-C_{16} molecules (Figure 2a). We note that the curves are steeper at the end of the compression and each of the isotherms is essentially shifted toward larger areas per molecule in the presence of HPA. It was proposed that the HPA molecules are situated in the middle of OMA-C_{16} and ODA molecules to form alternate lamellar structures with an increased molecular area (vide infra). Compared with the Keggin-type polyoxometalates $HPMo_{12}$ and HPW_{12}, the Dawson-type species HP_2Mo_{18} has more charges and bigger volume, which can result in a larger molecular area. Typical isotherms were also observed for the OMA-C_8 case (Figure 2b).

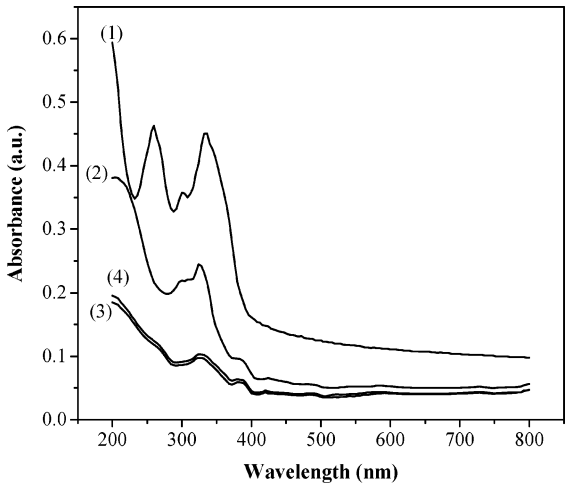

Figure 3. UV−vis spectra of LB films (13 layers) of (1) OMA-C_{16}/ODA/H_2O, (2) OMA-C_{16}/ODA/$HPMo_{12}$, (3) OMA-C_{16}/ODA/HP_2Mo_{18}, and (4) OMA-C_{16}/ODA/HPW_{12}.

Table 2. Absorption Data for the LB Films

LB film	λ_{max} (nm)
OMA-C_{16}/ODA/H_2O	302, 334, 368
OMA-C_{16}/ODA/$HPMo_{12}$	304, 332, 384
OMA-C_{16}/ODA/HP_2Mo_{18}	328, 384
OMA-C_{16}/ODA/HPW_{12}	328, 384
OMA-C_8/H_2O	312, 344, 360
OMA-C_8/$HPMo_{12}$	312, 336, 364
OMA-C_8/HP_2Mo_{18}	312, 348, 376
OMA-C_8/HAs_2W_{18}	304, 348, 382

UV−Vis Spectroscopy of LB Films. OMA-C_{16}/ODA/HPA of 13 layers and OMA-C_8/HPA of 9 layers LB films of high morphological stability were successfully deposited onto quartz substrates by the vertical method. The transfer ratio was almost unity in both dipping and lifting processes, indicating the formation of Y-type LB films. As shown in Figure 3, OMA-C_{16}/ODA/H_2O and OMA-C_8/H_2O films display strong absorption bands in the near UV region. These bands are mainly associated with the organic$^1(\pi\pi^*)$ transitions, possibly with some admixture of mercury atom orbitals, and the 0−0 absorption peak is assigned as the $S_0 \rightarrow S_1$ transition.[14] For OMA-C_{16}/ODA/HPA hybrids, the LB films exhibit intense O_d−M (M = Mo, W, 270 nm) and $O_{b(c)}$−M (330 nm or so) peaks which are perhaps mixed with organic$^1(\pi\pi^*)$ transitions (where O_d represents the terminal oxygen atoms whereas $O_{b(c)}$ the two different types of bridging oxygen atoms in HPA). Compared with OMA-C_{16}/ODA/H_2O, the absorption peaks of OMA-C_{16}/ODA/HPA LB films are slightly red-shifted which are presumably due to the delocalized π-conjugation caused by OMA and HPA. For OMA-C_8/HPA hybrids, the red shift of the absorption peaks of OMA-C_8/HPA was also observed with respect to that of OMA-C_8/H_2O. See Table 2.

Photoluminescence Properties of LB Films. With this method, luminescent LB films with OMA have been prepared. The photoluminescence (PL) spectra of the LB films (13 layers for OMA-C_{16} and 9 layers for OMA-C_8) deposited on quartz were measured, with the excitation wavelength at 330 nm (Figure 4). We observe broad intraligand-based$^1(\pi\pi^*)$ emission peaks in the range of 428−494 nm for each of them which arise from a singlet excited state (S_1). The emission patterns of all the films appear broad and unstructured at room temperature, which are characteristic of an aggregate or excimer site that is caused by the intermolecular mercurophilic interactions among the neighboring mercury centers.[14e,15] Such claim was possibly explained by X-ray crystallography and aggregation-induced absorption studies for OMA-C_8. The lattice of OMA-C_8 is characterized by the exhibition of various weak intermolecular Hg···Hg contacts of 3.738−4.183 Å, linking the individual molecular entities together to give a loose polymeric 3D structure (Figure 5). Examination of the absorption behavior of OMA-C_8 in $CHCl_3$ upon the addition of a nonsolvent MeOH also corroborates the presence of solid-state aggregates in thin films. While the amount of MeOH added is continuously increased at the expense of $CHCl_3$, a new band in the lower lying regime at 365 nm develops clearly, which corresponds to the lowest energy absorption peak observed in the solid state (Figure 6). Similar solid-state phenomenon is also commonplace for many mercury acetylides,[16] and in several occasions, such noncovalent metallophilicity turns out to be the major driving force toward supramolecular aggregation.[17] Interestingly, inclusion of HPA within the LB films causes important changes in their luminescence properties compared with those observed

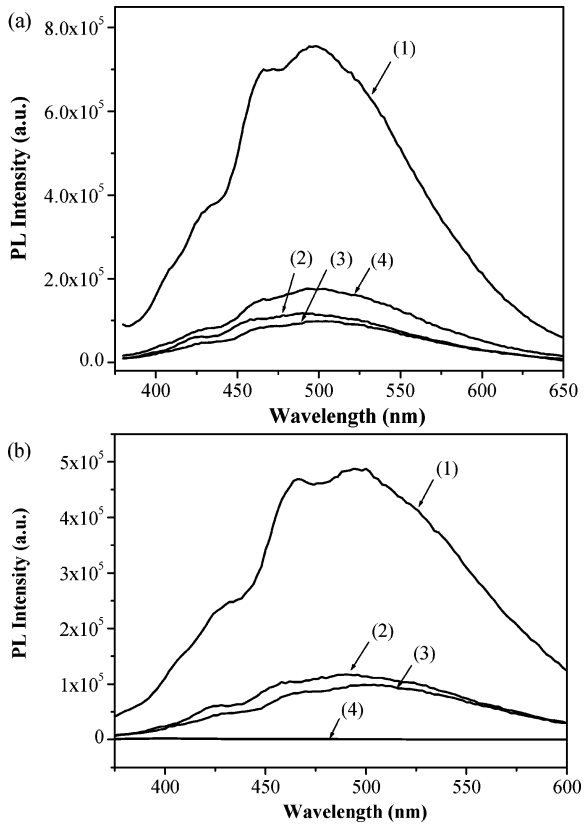

Figure 4. PL spectra of (a) 13-layer LB films of (1) OMA-C_{16}/ODA/H_2O, (2) OMA-C_{16}/ODA/$HPMo_{12}$, (3) OMA-C_{16}/ODA/HP_2Mo_{18}, and (4) OMA-C_{16}/ODA/HPW_{12} and (b) 9-layer LB films of (1) OMA-C_8/H_2O, (2) OMA-C_8/$HPMo_{12}$, (3) OMA-C_8/HP_2Mo_{18}, and (4) OMA-C_8/HAs_2W_{18}.

(15) (a) Liu, L.; Wong, W.-Y.; Poon, S.-Y.; Shi, J.-X.; Cheah, K.-W.; Lin, Z. *Chem. Mater.*, **2006**, *18*, 1369. (b) Wong, W.-Y.; Liu, L.; Poon, S.-Y.; Choi, K.-H.; Cheah, K.-W.; Shi, J.-X. *Macromolecules* **2004**, *37*, 4496. (c) Pschirer, N. G.; Bunz, U. H. F. *Macromolecules* **2000**, *33*, 3961. (d) Bunz, U. H. F. *Chem. Rev.* **2000**, *100*, 1605.

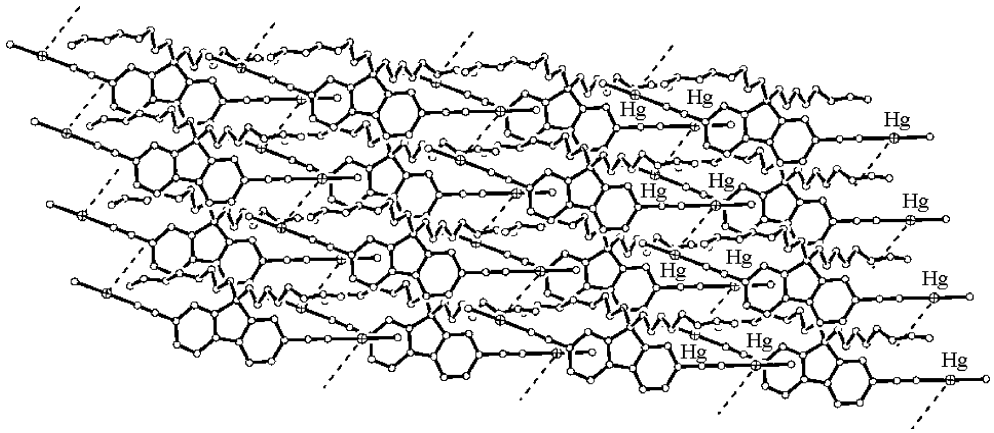

Figure 5. Solid-state packing diagram of OMA-C_8 showing the apparent mercurophilic interactions among Hg atoms in the crystal lattice.

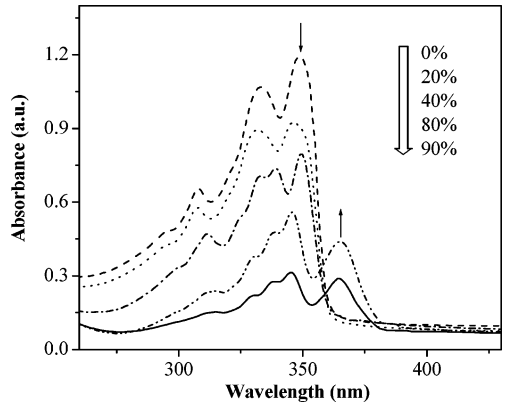

Figure 6. Aggregation-induced absorption spectra of OMA-C_8 at various volume ratios of $CHCl_3$/MeOH.

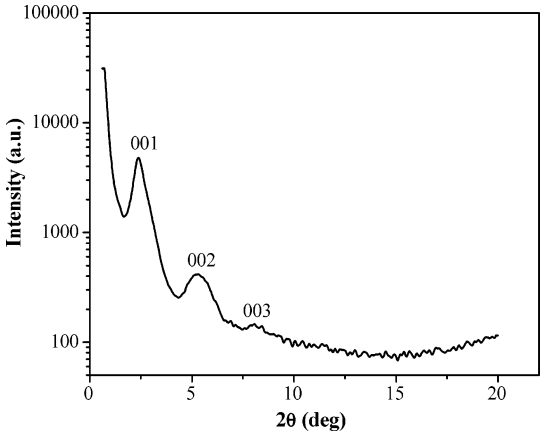

Figure 7. Low-angle X-ray diffraction pattern of the as-prepared OMA-C_{16}/ODA/$HPMo_{12}$ LB film with 13 layers deposited on glass. Indices for the Bragg reflections are also shown.

on pure water. For hybrid LB films of OMA-C_{16}/ODA/HPA and OMA-C_8/HPA, the PL intensity is lower than that of the OMA-C_{16}/ODA/H_2O and OMA-C_8/H_2O systems, respectively, and it is found that HPA quenches the luminescence of OMA to a certain extent.

Low-Angle X-ray Diffraction. The lamellar structure of the hybrid LB films can be clearly demonstrated by the low-angle X-ray diffraction experiment. Take OMA-C_{16} as an example; three Bragg peaks are clearly identified in the X-ray diffractogram of a 13-layer OMA-C_{16}/ODA/HPW_{12} LB film (Figure 7). The peaks at 2.39°, 5.26°, and 8.01° (2θ) correspond to the {001}, {002}, and {003} reflections, respectively, revealing a highly ordered stacking of different layers. According to the Bragg diffraction formula, $n\lambda = 2d \sin\theta$, we can calculate the monolayer average thickness $2/d$ to be 1.85 nm. The periodicity of the layered structure deduced from this experiment is ca. 3.7 nm. It is known that the length of the ODA molecule with a trans zigzag conformation is 2.4 nm,[18] whereas those of OMA-C_{16} and Keggin HPA molecules are 2.2 nm[14e] and 1 nm,[10] respectively. The total length of the three molecules arranged layer by layer is ca. 5.6 nm, which is larger than the calculated d value (3.7 nm). Our X-ray diffraction results are consistent with the lamellar layered structure for the OMA-C_{16}/ODA/$HPMo_{12}$ LB film (Figure 8) in which the three molecules lay down at some angles with the interfacial planes.

Atomic Force Microscopy. Surface characterization of the LB films by atomic force microscopy (AFM) has also been performed. The image and structure of the hybrid monolayer film deposited on mica was measured (Figure 9). The AFM image of OMA-C_{16}/ODA/$HPMo_{12}$ (Figure 9a) shows that the hybrid LB film consists of disperse particles with different domain sizes of 0.60−3.96 nm. The average surface roughness (R_a) is 2.7 nm and the largest roughness (R_z) is 3.6 nm. A dimensionally split phase structure can be observed in which the darker area is mostly filled with HPA and the higher and brighter area is mostly filled with OMA-C_{16}/ODA. The topographic and cross-sectional image of OMA-C_8/$HPMo_{12}$ monolayer film is shown in Figure 9b with the R_a and R_z values of 0.5 and 14.8 nm, respectively.

Surface Photovoltage Spectroscopy. The photovoltaic effect of the 13-layer hybrid LB films deposited on the silica

(16) (a) Liu, L.; Poon, S.-Y.; Wong, W.-Y. *J. Organomet. Chem.* **2005**, *690*, 5036. (b) Wong, W.-Y.; Choi, K.-H.; Lu, G.-L.; Lin, Z. *Organometallics* **2002**, *21*, 4475. (c) Wong, W.-Y.; Lu, G.-L.; Liu, L. Shi, J.-X.; Lin, Z. *Eur. J. Inorg. Chem.* **2004**, 2066. (d) Liu, L.; Wong, W.-Y.; Shi, J.-X.; Cheah, K.-W. *J. Polym. Sci., Part A: Polym. Chem.* **2006**, *44*, 5588. (e) Liu, L.; Wong, W.-Y.; Shi, J.-X.; Cheah, K.-W.; Lee, T.-H.; Leung, L.-M. *J. Organomet. Chem.* **2006**, *691*, 4028. (f) Poon, S.-Y.; Wong, W.-Y.; Cheah, K.-W.; Shi, J.-X. *Chem. Eur. J.* **2006**, *12*, 2550. (g) Faville, S. J.; Henderson, W.; Mathieson, T. J.; Nicholson, B. K. *J. Organomet. Chem.* **1999**, *580*, 363.

(17) (a) Pyykko, P. *Chem. Rev.* **1997**, *97*, 597. (b) Rais, D.; Mingos, D. M. P.; Vilar, R.; White, A. J. P.; Williams, D. J. *Organometallics* **2000**, *19*, 5209. (c) Mingos, D. M. P.; Vilar, R.; Rais, D. *J. Organomet. Chem.* **2002**, *641*, 126.

(18) Takahashi, M.; Kobayashi, K.; Takaoka, K. *Langmuir* **2000**, *16*, 6613.

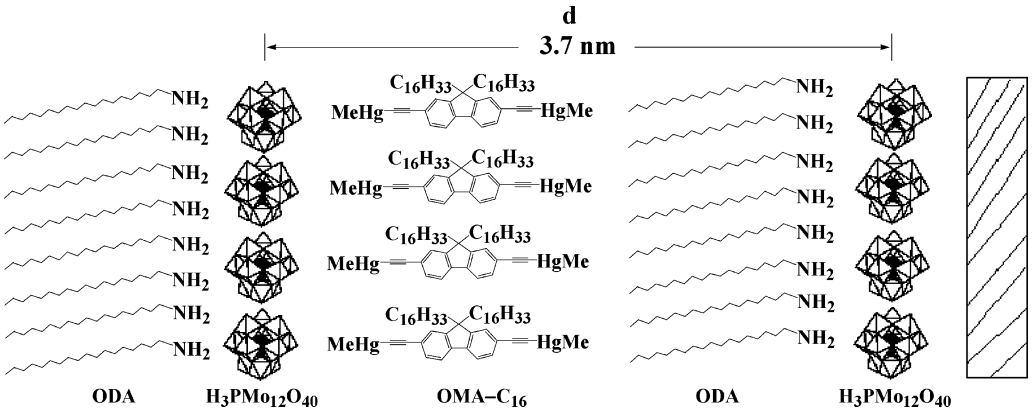

Figure 8. Schematic representation of the proposed structure of the OMA-C_{16}/ODA/$H_3PMo_{12}O_{40}$ nanohybrid LB film.

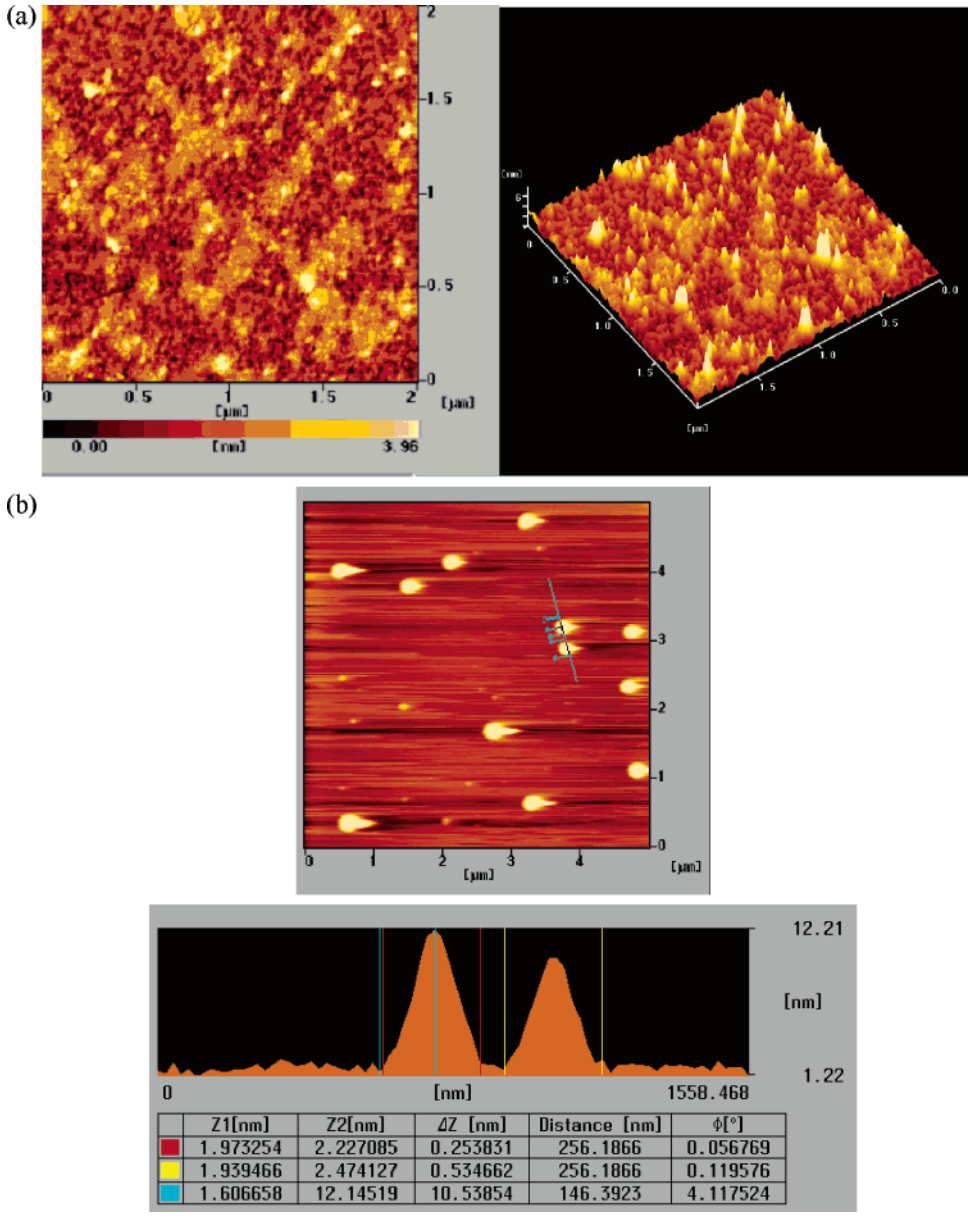

Figure 9. (a) Tapping mode AFM image of the OMA-C_{16}/ODA/$HPMo_{12}$ monolayer film and (b) AFM topography image (upper) and section profile (lower) of the OMA-C_8/$HPMo_{12}$ monolayer film.

wafer was also studied after UV-irradiation using the surface photovoltage spectroscopy (SPS) technique. The results are shown in Table 3 and Figure 10. The impact of mercury acetylides in photovoltaic phenomenon is well-illustrated in the present study. The OMA-C_{16}/ODA/H_2O and OMA-C_{16}/ODA/HPA hybrid LB films display strong photovoltage effect in the near UV region. The photovoltage performance generally follows the order OMA-C_{16}/ODA/$HPMo_{12}$ >

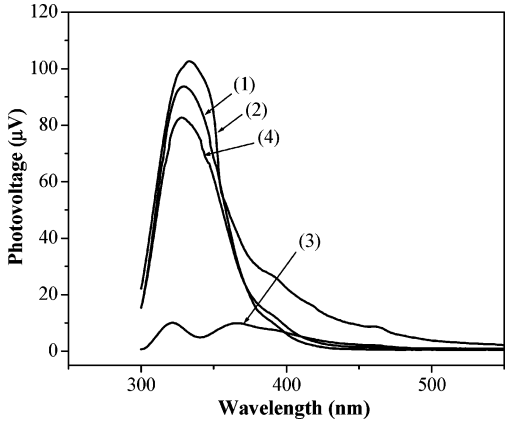

Figure 10. Surface photovoltage responses of hybrid LB films (13 layers) of (1) OMA-C_{16}/ODA/H_2O, (2) OMA-C_{16}/ODA/$HPMo_{12}$, (3) OMA-C_{16}/ODA/HP_2Mo_{18}, and (4) OMA-C_{16}/ODA/HPW_{12}.

Table 3. Surface Photovoltage Spectroscopic Data for Various LB Films

LB film	λ (nm)	V (μV)
OMA-C_{16}/ODA/H_2O	329	93.7
OMA-C_{16}/ODA/$HPMo_{12}$	333	102.7
OMA-C_{16}/ODA/HP_2Mo_{18}	321	10.1
	365	9.9
OMA-C_{16}/ODA/HPW_{12}	328	82.7

OMA-C_{16}/ODA/H_2O > OMA-C_{16}/ODA/HPW_{12} > OMA-C_{16}/ODA/HP_2Mo_{18} and the photovoltage responses can be as high as 102.7 μV. It is known that mercury acetylide complex which contains π-conjugated electrons can serve as a $\sigma-\pi$ electron donor, whereas the three types of HPA are photosensitive substances and act as electron acceptors. With this concept, our OMA/ODA/HPA hybrid system can manifest donor$-\pi-$acceptor (D$-\pi-$A) structural motif and the π-conjugated system can be used as an electron-transporting passage. When the LB film was excited by light, the photovoltaic effect readily comes into play. The structure of the film does permit electron delocalization to an appreciable extent. It was found that a change in the metal type from Mo to W ((2) vs (4) in Figure 10) caused a noticeable decrease in the photovoltage at a given wavelength. Moreover, heteropolyoxomolybdates of the Keggin-type exhibit the highest photovoltage values while the Dawson-type gives the lowest photovoltage response ((2) vs (3) in Figure 10). Presumably, the rugby-shaped HP_2Mo_{18} tends to be less effective in self-organizing with OMA relative to the more spherical-like $HPMo_{12}$. In addition, it is believed that charge transfer can take place between the interface of the title LB film and *p*-Si substrate.[19] The adsorption of polyoxometalate anions along a ODA monolayer must be induced by electrostatic interactions between the ion and the charge density at the interface. Accordingly, free-standing films containing alkynylmercury complexes can be prepared by electrostatic layer-by-layer assembly.

Electrical Characterization of Monolayer LB Films by Scanning Tunneling Microscopy. The electric conductivity behavior of OMA-C_8/HP_2Mo_{18} monolayer film on silica wafer was examined using scanning tunneling microscopy. When the voltage is monitored at $\pm$10 V, the tunneling current obtained is 0.08 to ca. $-$0.92 nA. This value only shows a slight increase as compared with that for OMA-C_8/H_2O (0 to ca. $-$0.92 nA). Remarkably, for OMA-C_8/HAs_2W_{18} monolayer film, it can show good electrical conductivity, and the tunneling current amounts to $\pm$100 nA when the voltage is set at $\pm$3 V. A representative $I-V$ plot is shown in Figure 11 for such a device. It should be noted that OMAs are very poor conductors in the intrinsic state but our hybrid LB composite in the device can be semiconducting. The largest conductance of the device is about 0.17 $\times$ 10^{-6} S at $-$1.6 V.

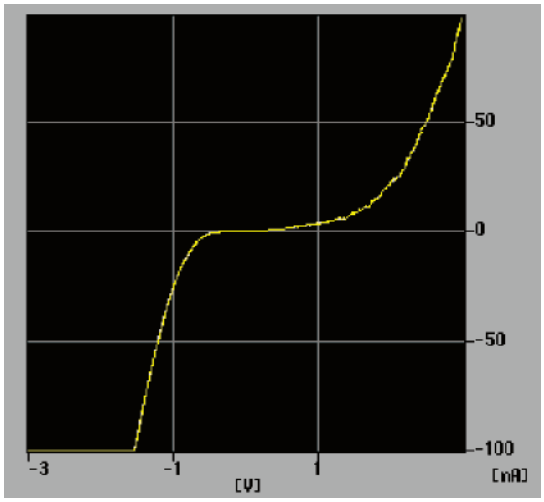

Figure 11. $I-V$ curve of OMA-C_8/HAs_2W_{18} monolayer film on the silica wafer.

Concluding Remarks

This study has demonstrated that mercury acetylides can be used to build new organometallic/inorganic superlattices useful for photoelectric applications. These compounds can form steady monolayers and multilayers at the interface of air and heteropolyacid aqueous solutions. This is the first observation of periodicity of OMA molecules in built-up LB films. Because of the charge transfer between mercury acetylide donor and heteropolyacid acceptor as well as the possible hydrogen-bonding network formation and adsorption phenomenon, the films can be significantly compressed and aggregated in the solid region and Y-type photovoltaic nanohybrid LB films have been prepared. By virtue of the D$-\pi-$A structure for the films, photoconductivity was easily observed upon photoexcitation. Organomercury acetylides allow a delocalized electron transfer in the large π-conjugated bond system, leading to good electrical conductivity in the LB films.

For the hybrid LB films based on OMA, weak $d^{10}\cdots d^{10}$ mercurophilic interaction, $\pi-\pi^*$ transition between the triple bond of OMA and the aromatic system of the ligand, and electron transfer between electron donor and acceptor are believed to be the main causes for the good photovoltaic effect of the title hybrid LB films. Such an organic/organometallic/inorganic multifunctional assembly gives rise to new ultrathin materials. The work can be

(19) Zhang, W. F.; Guo, H.; Ma, G. H.; Huang, Y. B.; Du. Z. L. *Chem. J. Chin. Univ.* **1997**, *19*, 591.

further extended to different kinds of polyoxometalate clusters, possibly affording new lamellar materials. In fact, a correct choice of polyoxometalate allows the elaboration of LB films exhibiting particular surface and optoelectronic properties. Precise construction of a thin film of polyoxometalate is desired for realizing practical molecular functional devices. Obviously, the occurrence of photoluminescent activity confirms the potential for creating light-emitting multilayer films with OMA and HPA.

Acknowledgment. The authors acknowledge the financial support from the National Natural Science Foundation of China (20671033), the Hong Kong Research Grants Council (HKBU 2022/03P), and Hong Kong Baptist University.

CM062838C